

# Numerical Investigations of parabolic trough collectors using different nanofluids

Nabeel Abed  
Department of Mechanical, Aerospace,  
and Civil (MACE) engineering, school of  
Engineering  
University of Manchester  
Manchester, UK  
nabeel.abed@manchester.ac.uk

Hector Iacovides  
Department of MACE, school of  
Engineering  
University of Manchester  
Manchester, UK  
h.iacovides@manchester.ac.uk

Imran Afgan  
Department of Mechanical Engineering,  
College of Engineering, Khalifa University of  
Science and Technology, Abo Dhabi, UAE,  
imran.afgan@ku.ac.ae  
Department of MACE, school of Engineering  
University of Manchester, Manchester, UK  
imran.afgan@manchester.ac.uk

Andrea Cioncolini  
Department of MACE,  
school of Engineering  
University of Manchester  
Manchester, UK  
andrea.cioncolini@manchester.ac.uk

Adel Nasser  
Department of MACE, school of  
Engineering  
University of Manchester  
Manchester, UK  
a.g.nasser@manchester.ac.uk

Tarek Abdel-Malak Meakhail  
Department of Mechanical Engineering,  
Faculty of Energy Engineering- Aswan  
University  
Aswan, Egypt.  
TMalak@aswu.edu.eg

**Abstract**— This paper presents three dimensional numerical simulations of parabolic trough collectors (PTC) based on two low-Reynolds eddy viscosity turbulence models, namely; Launder and Sharma k-epsilon and k-omega SST models. For the simulations, water was used as the Heat Transfer Fluid (HTF) with four different nanoparticles; Al<sub>2</sub>O<sub>3</sub>, TiO<sub>2</sub>, CuO and Cu. Different volume fractions ( $\phi$ ) of the nanoparticles were investigated for various Reynolds (Re) numbers with uniform heat flux. Results showed that the overall performance of the system is more sensitive to changes in the thermal properties of nanofluid than the thermal properties of the HTF. At a volume fraction of 6% and a Re number of 70,000, the Nusselt number (Nu) enhancement of nanofluids TiO<sub>2</sub>-water, Al<sub>2</sub>O<sub>3</sub>-water, CuO-water and Cu-water were found to be 21.5%, 20.2%, 18.11% and 15.7% respectively while the performance evaluation criteria (PEC) were 1.214, 1.2, 1.18 and 1.155 respectively.

**Keywords**—Nanofluids, parabolic trough collector; passive heat transfer enhancements; solar thermal energy.

## I. INTRODUCTION

To tackle the climate change and global warming, the world needs to reduce its dependency on fossil fuels. In recent years, clean renewable and sustainable sources of energy such as solar, wind, tidal etc. have thus become widely popular. In particular, solar thermal energy has emerged as a major contender in the quest to reduce CO<sub>2</sub> emissions especially for regions with hot tropical climate. The light or solar energy/heat from the sun can be harnessed to produce electricity via Photovoltaic Devices (PV) or Concentrating Solar Power (CSP) plants. The CSP plants operate on Direct Normal Irradiance (DNI), which is defined as the amount of received solar energy per unit area on the surface held normal to the rays of the sun. Depending upon the methodology to capture the suns energy, the CSP technology can be categorized into several technologies, four of the most common ones being; parabolic trough collectors (PTC: which is our focus), linear Fresnel reflectors, parabolic dishes and solar towers.

The PTC system consists mainly of three important sub-systems; the solar field systems, the storage system and the

power block system. The solar field sub-system can be categorized as a type of a large heat exchanger with the main components being the solar collector and the reflector surface. The reflector surface is generally made up of a series of mirrors that directs the solar energy to the solar collector. The solar collector then converts the absorbed incident solar radiation into thermal energy which is carried through the collector via the Heat Transfer Fluid. Within the solar collector, an absorber tube is generally made from a metal which is coated with black color to achieve larger solar absorbance and to reduce the thermal emittance. The absorber tube is encased within a glass envelope which is itself covered with an anti-reflective coating to reduce the heat losses by convection.

## II. THERMAL PERFORMANCE OF PTCs

The absorber tube (it is referred also to heat collection element (HCE)) is one of the most important elements in a PTC system. A high efficiency of the absorber tube means higher thermal efficiency, lower plant costs and a lower temperature gradient of absorber tube; all of these lead to a better plant reliability. Because of these advantages, four main technologies of heat transfer enhancement have been considered particularly within the absorber tube. The thermal performance of a PTC can be improved by either changing the heat transfer fluid or by adding nanoparticles (metallic or non-metallic) to it thus enhancing its thermal properties. The possible third technology is to insert swirl generators inside the HCE to enhance the heat augmentation. The fourth technique is to use inserts within the HCE using nanofluids.

## III. THERMAL PERFORMANCE BY ADDING NANOPARTICLES

One of the most useful techniques used to improve the thermal performance in PTCs is to add metallic or non-metallic nanoparticles inside the base working fluid which in turn leads to creation of the medium called nanofluid. The main function of nanofluid in solar fields is to capture the solar energy in such a way that it is more effective than the

base fluid leading to improvement in the thermal performance of the absorber. Increasing the  $\phi$  of the nanoparticles not only enhances the convection heat transfer but also decreases the thermal stresses on the absorber tube. However, an increase in the nanoparticle density may lead to their agglomeration in certain areas thus raising the pressure required to pump the fluid. Thus, one needs to optimize the  $\phi$  ratio of nanoparticles for heat transfer enhancement.

There are two entirely different approaches to modelling the nanofluids; either as a single-phase or a two-phase model. Both these approaches have successfully been used in the past with the two-phase approach being costly but more accurate. Furthermore, accurate numerical predictions depend heavily on the selection of the thermos-physical properties of the nanoparticles. Various theoretical forms of their thermos-physical properties are available in the literature along with some correlations as presented in [1].

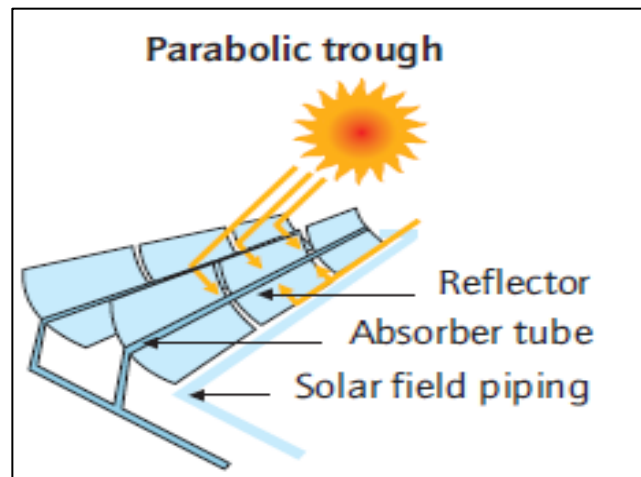
#### IV. LITERATURE REVIEW OF NANOFLUIDS IN PTCs

Reference [2] used  $Al_2O_3$  in Ionic Liquids with various values of  $\phi$  (0.9, 0.18 and 0.36) reported enhancement of thermal conductivity by 11% and heat capacity by 49% for  $\phi=0.9$ . Using both single and two phase modelling approaches by [3] reported a 36% increase in the heat transfer coefficient with  $Al_2O_3$  immersed in synthetic oil at  $\phi$  of 5%. Reference [4] examined the effect of mixed nanoparticles of  $CuO-Al_2O_3$  in water with different ratios of  $\phi$ . The optimum values of PH, sonication time, and mass concentration were 7.5-8.5, 100-120 min and 1.25 which lead to the maximum level of repulsive and dispersion forces between the nanoparticles. In 2017, [5] used the same nanoparticles but with two different base fluids (Water and water-EG (ethylene glycol)) with  $\phi$  of 0.05, 0.1 and 0.2%. According to their findings the thermal efficiency was higher for pure water since the mixture of water-EG had much higher boiling and freezing temperatures. Another issue highlighted by [6] is that the absorber deformation decreased substantially from 2.11 mm to 0.54 mm when  $\phi$  was increased from 0 to 0.05% for  $Al_2O_3$ -synthetic oil. Reference [7] used another type of nanofluids (Cu- Therminol<sup>®</sup>VP-1) and reported heat transfer enhancements of 8%, 18% and 32% at  $\phi$  of 2%, 4% and 6% respectively. Recently, [8] used metallic and non-metallic nanoparticles in Syltherm 800-base fluid with  $\phi$  of (3 and 5%). The authors reported the relative gain in thermal energy were 1.46, 1.25 and 1.4 for  $Al_2O_3$ ,  $CuO$  and  $TiO_2$  respectively. However, the maximum exergy efficiency obtained was about 9.05% by using 3% of  $CuO$ . Reference [9] used another type of non-metallic nanoparticle,  $NiO$  immersed in biphenyl and diphenyl oxide. This resulted increasing the heat transfer coefficient by 50% and thermal conductivity by 96%. In the present work, the metallic and non-metallic nanoparticles (Alumina ( $Al_2O_3$ ), Copper oxide ( $CuO$ ), Titanium Oxide ( $TiO_2$ ) and Copper ( $Cu$ )) are immersed in water with different  $\phi$  and Re numbers under uniform heat flux in the circumferential direction.

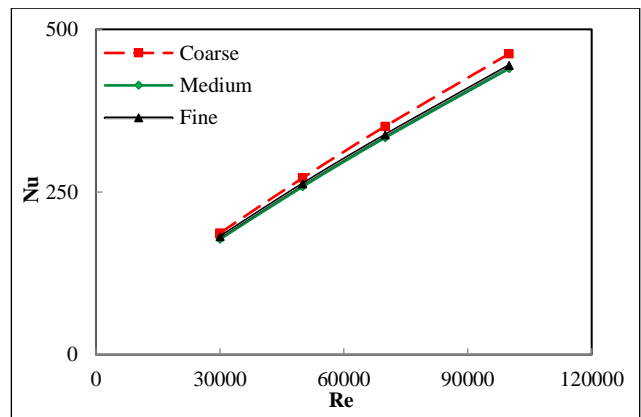
#### V. SOLAR RECEIVER

In this section we present the CFD results of a solar absorber of 2m length and 60mm diameter, as shown in “Fig. 1a”. Open source solver, OpenFOAM, was used to study flow

characteristics and heat transfer utilizing two low-Reynolds turbulence models; Launder and Sharma  $k-\epsilon$  and Shear Stress transport  $k-\omega$  models. For the simulations, the heat flux ( $q$ ) was fixed at 50000 “W/m<sup>2</sup>”. The base fluid and nanofluid were incompressible and the effect of gravity was neglected. Three different meshes were tested for the mesh independence study; Coarse (0.5 million cells), Medium (1.3 million cells) and Fine (2.1 million cells). For all grids the near wall non-dimensional distance was kept at a  $Y^+$  of 1 to resolve the viscous sublayer. A comparison of the Nu number with the Re number is shown in “Fig 1b” for all the three meshes. From the “Fig. 1b” it can be observed that the medium grid is sufficient for the present study as further mesh refinement had almost no effect on the Nu number profile.



(a)



(b)

Fig. 1. (a) Schematic of the parabolic trough receiver, (b) Mesh independence study for three different grids.

#### A. Boundary conditions

The boundary conditions (BC's) used in the present study are listed in “Table 1”.

**Table 1:** boundary conditions applied in the present work.

| BC's  | U (m/s)     | P (Pa)    | T (K)                 | K ( $m^2/s^2$ ) | $\epsilon$ ( $m^2/s^3$ ) | $\omega$ (1/s)   |
|-------|-------------|-----------|-----------------------|-----------------|--------------------------|--|
| inlet | Fixed Value | Zero grad | Fixed Value           | Fixed Value     | Fixed Value              | Fixed Value  |
| wall  | No-slip     | Zero grad | q (W/m <sup>2</sup> ) | Zero            | Zero                     | Fixed Value<br>$\omega = \frac{60 \nu}{0.75 (\Delta y)^2}$ |

|        |            |      |            |            |            |            |
|--------|------------|------|------------|------------|------------|------------|
| outlet | Zero grad. | Zero | Zero grad. | Zero grad. | Zero grad. | Zero grad. |
|--------|------------|------|------------|------------|------------|------------|

### B. Thermo-physical properties of nanofluid

In the present study, a single-phase modelling method is used to model the nanofluid which is based on the physics of mixture of two different materials; a base fluid of water at  $T=320.15\text{K}$  mixed sequentially with four different nanoparticles ( $\text{Al}_2\text{O}_3$ ,  $\text{CuO}$ ,  $\text{TiO}_2$  and  $\text{Cu}$ ). Their properties (density,  $\rho$  ( $\text{kg/m}^3$ ), thermal conductivity,  $k$  ( $\text{W/m.K}$ ), specific heat capacity,  $C_p$  ( $\text{J/kg.K}$ ) and dynamic viscosity,  $\mu$  ( $\text{N.s/m}^2$ )) at the ambient temperature are listed in “Table 2”. Three different  $Re$  numbers were considered for the present study (30,000, 50,000 and 70,000) and three values of  $\phi$  (2%, 4% and 6%).

Table 2: Thermal properties of water and various tested nanoparticles, [10].

| Property                   | water   | $\text{Al}_2\text{O}_3$ | $\text{CuO}$ | $\text{TiO}_2$ | $\text{Cu}$ |
|----------------------------|---------|-------------------------|--------------|----------------|-------------|
| $\rho$ ( $\text{kg/m}^3$ ) | 988.9   | 3970                    | 6320         | 4250           | 8933        |
| $k$ ( $\text{W/m.K}$ )     | 0.6398  | 40                      | 77           | 8.95           | 401         |
| $C_p$ ( $\text{J/kg.K}$ )  | 4180.4  | 765                     | 532          | 686            | 385         |
| $\mu$ ( $\text{N.s/m}^2$ ) | 0.00058 | -                       | -            | -              | -           |

The single-phase approach is reasonably accurate when  $\phi$  of the nanoparticles is smaller than 10% and the diameter of nanoparticles is less than 100 nm, [7]. In this approach, the nanofluid density ( $\rho_{nf}$ ) is calculated depending on the classical form of heterogeneous mixture. Whereas, the specific heat capacity ( $C_{p,nf}$ ) was determined depending on the thermal equilibrium between the solid particles and surrounding base fluid. However, several models were used for determining the nanofluid viscosity and thermal conductivity and the most appropriate models are used in the present work.

$$\rho_{nf} = (1 - \phi)\rho_b + \phi\rho_p \quad (1)$$

$$C_{p,nf} = \frac{(1 - \phi)\rho_b C_{p,b} + \phi\rho_p C_{p,p}}{\rho_{nf}} \quad (2)$$

$$\mu_{nf} = \mu_b(123\phi^2 + 7.3\phi + 1) \quad (3)$$

$$k_{nf} = 0.25[(3\phi - 1)k_p + (2 - 3\phi)k_b + \sqrt{[(3\phi - 1)k_p + (2 - 3\phi)k_b]^2 + 8k_p k_b}] \quad (4)$$

Where the subscript ( $nf$ ) represents nanofluids, ( $p$ ) refers to the nanoparticle and ( $b$ ) the base fluid. The properties of nanofluids resulting from these equations are presented in “Fig. 2” which shows the Prandtl number ( $Pr = \mu_{nf} \cdot C_{p,nf} / k_{nf}$ ) for each of the nanofluid. The highest value of  $Pr$  number was observed for ( $\text{TiO}_2$ ).

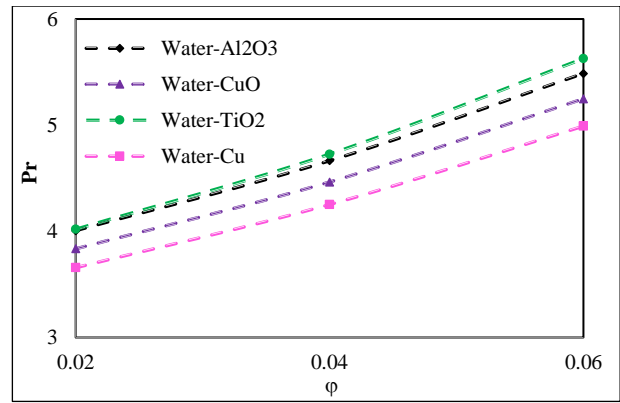
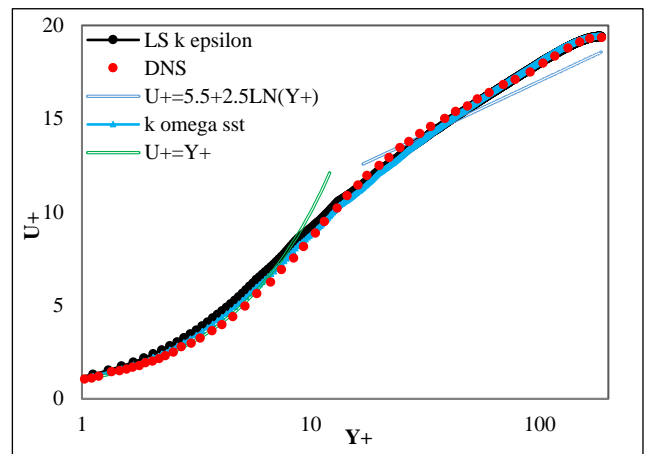


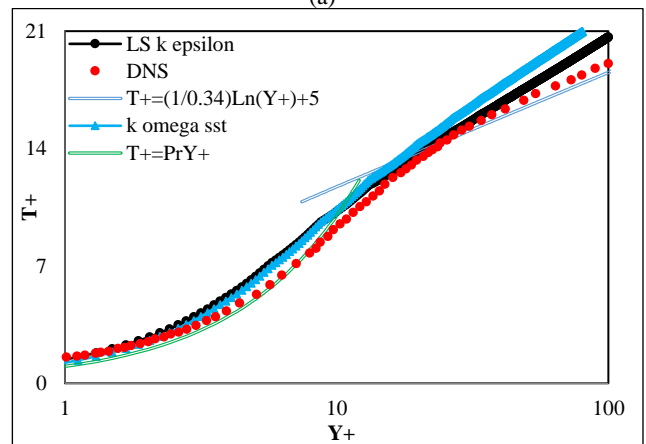
Fig. 2. The  $Pr$  number behaviour of nanofluids under consideration at  $T=320.15\text{K}$ .

### C. Model validation

Results are compared to the DNS data of [11] at a bulk  $Re$  of 5500 and  $Pr$  number of 1. The non-dimensional stream-wise velocity ( $U^+ = U/U_\tau$ ) of pure water and the dimensionless mean temperature ( $T^+ = (T_w - T)/T_\tau$ ) profiles are shown in “Fig. 3” where the friction velocity is defined as ( $U_\tau = \sqrt{\tau/\rho}$ ), where ( $\tau$ ) is the wall shear stress (Pa) and the friction temperature is defined as ( $T_\tau = q/\rho C_p U_\tau$ ). It was observed that both tested RANS model predictions were decent compared to the DNS of [11].



(a)



(b)

Fig. 3: Comparison between the dimensionless parameters with the DNS data of [11] (a) Mean velocity profile (b) Mean temperature profile.

The model predictions were also validated against the experimental correlation of [12] for Nu number and friction factor and with the experimental correlation of [13] for only Nu number. These correlations for the fully developed turbulent flow are respectively given by:

$$Nu = \frac{(f/8)Re}{1.07 + 12.7(f/8)^{0.5}(Pr^{2/3}-1)} \quad \text{for} \quad \begin{cases} 0.5 \leq Pr \leq 2000 \\ 10^4 < Re < 5 \times 10^6 \end{cases} \quad (5)$$

$$f = (0.79 \ln Re - 1.64)^{-2} \quad \text{for} \quad (3000 < Re < 5 \times 10^6) \quad (6)$$

$$Nu = \frac{(f/8)(Re-1000)}{1 + 12.7(f/8)^{0.5}(Pr^{2/3}-1)} \quad \text{for} \quad \begin{cases} 0.5 \leq Pr \leq 2000 \\ 3 \times 10^3 < Re < 5 \times 10^6 \end{cases} \quad (7)$$

It can be noticed from “Fig. 4” that the present CFD predictions by the SST k- $\omega$  model are better than those of LS k- $\epsilon$  model as it agrees well with the experimental correlations showing an error of only 6.1% for the Nusselt number and 7.5% for the friction factor.

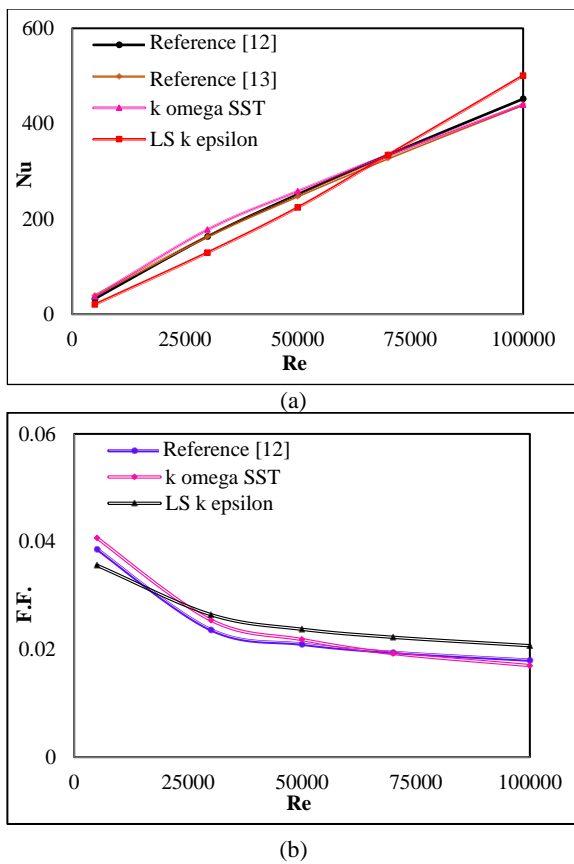


**Fig. 4.** Comparisons of current results with experimental correlations of [12] and [13] (a) Average Nu number (b) Friction factor

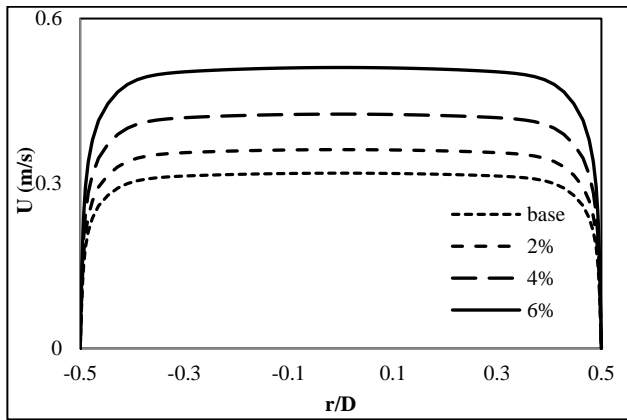
## VI. DISCUSSION OF RESULTS

The mean velocity profiles at Re=30,000 at the location of 1.75m for all types of nanofluids are presented in “Fig. 5”. It can be observed that by increasing the  $\phi$  of a particle, the velocity profiles become more uniform with a noticeable increase in regions away from the wall. However, at  $\phi=2\%$ , the increase in velocity is larger for water-Al<sub>2</sub>O<sub>3</sub> and water-TiO<sub>2</sub> than the other two nanofluids which becomes more prominent at higher ratios of  $\phi$ . On the other hand an opposite trend is observed for the temperature away from the walls,

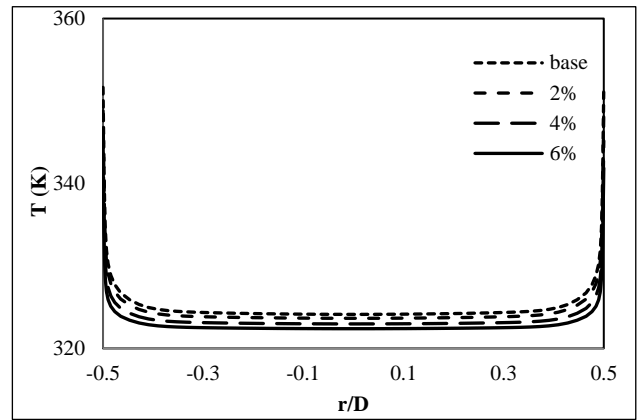
where for increasing the  $\phi$ , the temperature in the middle of the channel decreases. Again this decrease is more prominent for higher  $\phi$  as shown in “Fig. 6”.

The average Nu number in the parabolic trough receiver is given by ( $Nu = hD/k$ ) and the heat transfer coefficient by  $h = q/(T_w - T_b)$  where  $D$  is the receiver diameter,  $k$  the thermal conductivity,  $T_w$  the average wall temperature and  $T_b$  the average bulk temperature calculated as  $(T_{inlet} + T_{out})/2$ . The average Nu number profiles of the base fluid and nanofluids for all values of  $\phi$  is illustrated in “Fig. 7”. It can be observed that the Nu number increases as the  $\phi$  is raised. The positive slope in “Fig. 7” represents the behaviour of the ( $Pr$ ) number, as presented in “Fig. 2”. A similar trend is observed for increasing  $Re$  number which is due to the reduction in the thickness of the viscous sublayer. At a  $\phi$  of 6% and  $Re=70000$ , the Nu number enhancement of nanofluids water-TiO<sub>2</sub>, water-Al<sub>2</sub>O<sub>3</sub>, water-CuO and water-Cu are found to be 21.5, 20.2, 18.11 and 15.7% respectively. The pressure drop ( $\Delta P$ ) and Darcy friction factor ( $f$ ) in the parabolic trough receiver are respectively given by  $\Delta P = f \left(\frac{L}{D}\right) \left(\frac{\rho U_{ave}^2}{2}\right)$  and  $f = (8\tau_w)/(\rho U_{ave}^2)$ . The pressure drop in the solar receiver occurs due to the frictional force acting on the heat transfer fluid as it flows. The two factors directly affecting this frictional force are the flow velocity and the viscosity. According to the aforementioned equations, the frictional shear force and the pressure drop within the pipe are directly proportional. Therefore, the higher the shear force, the larger the pressure drop across the receiver section. This is confirmed by “Fig. 8” which presents the pressure drop of the base fluid and nanofluids for all the tested configurations. Here it can be noted that the pressure drop increases with both  $Re$  number and the  $\phi$  of the nanoparticles.

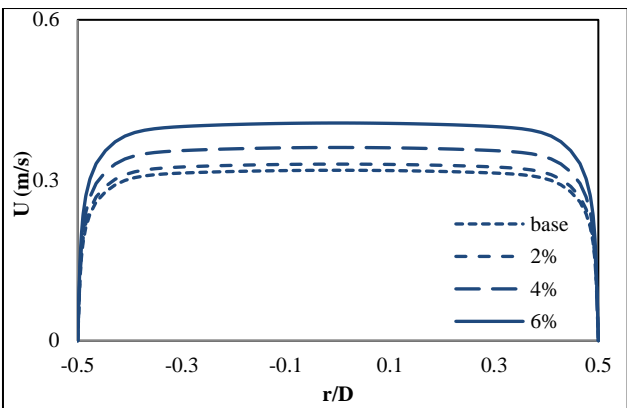
A comparison of (PEC) of all considered nanofluids is shown in “Fig. 9” which presents data at a  $Re$  number of 70,000 and  $\phi=6\%$ . This parameter can be calculated by ( $PEC = \frac{Nu}{Nu_o} / \left(\frac{f}{f_o}\right)^{1/3}$ ), where  $Nu_o$  is the Nu number and  $f_o$  the friction factor of the pure working fluid. Here a PEC value of more than 1, indicates an enhancement in the flow performance. Larger magnitudes of the PEC ( $>1$ ) indicate larger thermal performance of nanofluids under the same power pumping requirements. Considering this parameter, the largest value was recorded with TiO<sub>2</sub>-water for all the tested values of  $\phi$ . At a  $\phi$  of 6% and  $Re = 70000$ , the PEC of nanofluids water-TiO<sub>2</sub>, water-Al<sub>2</sub>O<sub>3</sub>, water-CuO and water-Cu were found to be 1.214, 1.2, 1.18 and 1.155 respectively.



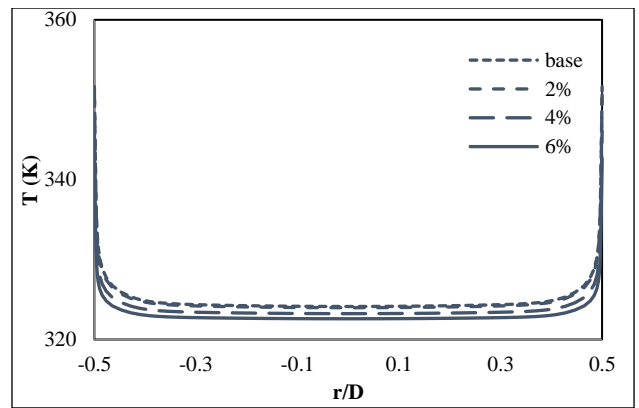
(a) water-Al<sub>2</sub>O<sub>3</sub>



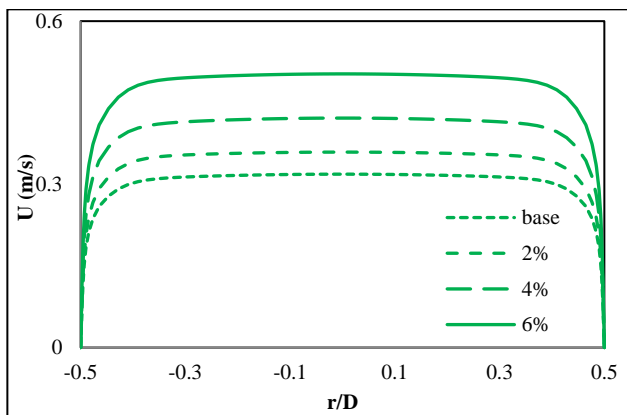
(a) water-Al<sub>2</sub>O<sub>3</sub>



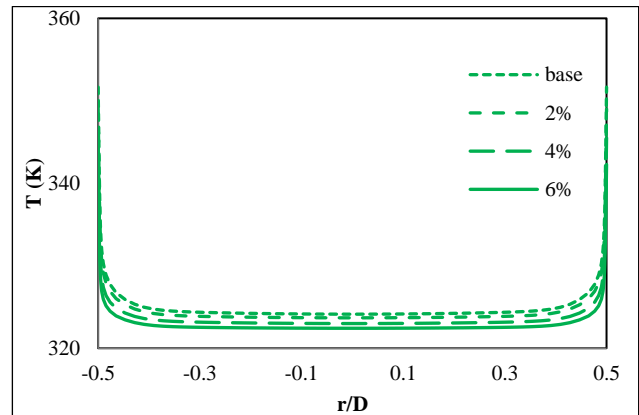
(b) Water-Cu



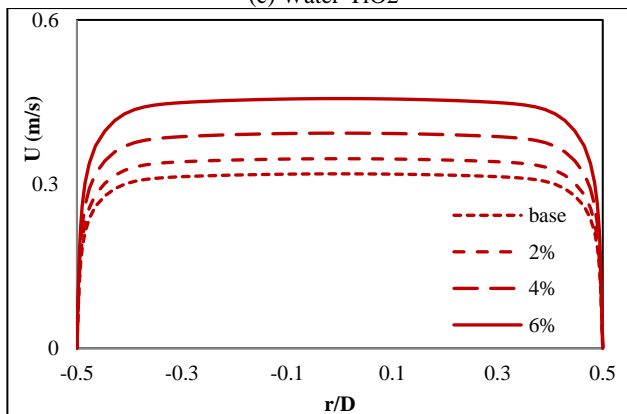
(b) Water-Cu



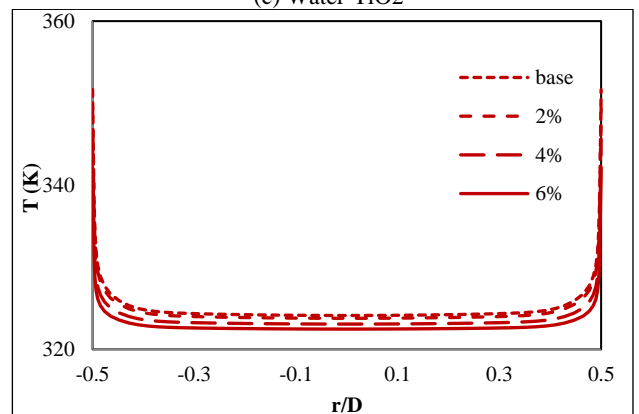
(c) Water-TiO<sub>2</sub>



(c) Water-TiO<sub>2</sub>



(d) Water-CuO

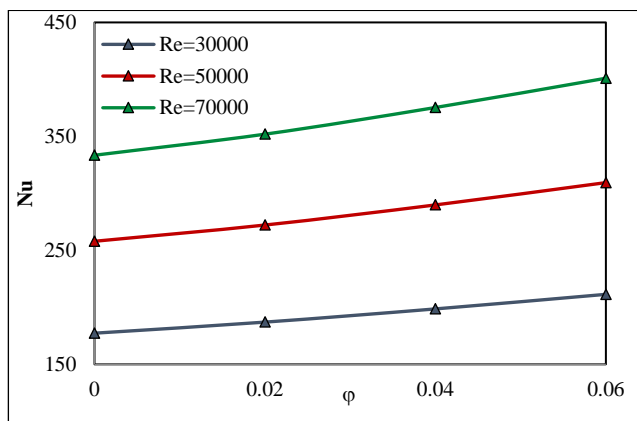


(d) Water-CuO

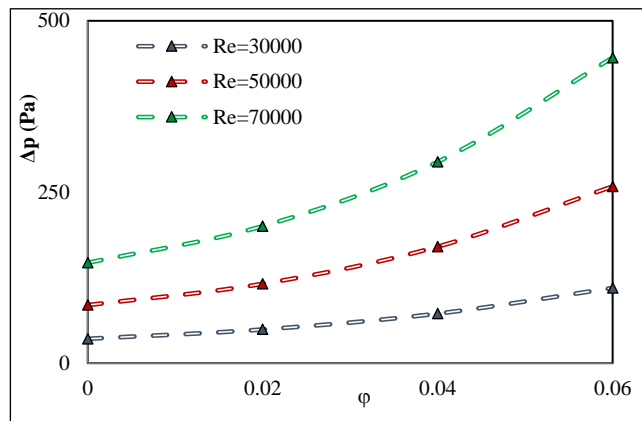
**Fig. 5.** Effect of particle loading on the mean velocity profiles at  $L=1.75\text{m}$  and  $Re=30,000$ .

**Fig. 6.** Effect of particle loading on the mean temperature profiles at  $L=1.75\text{m}$  and  $Re=30,000$ .

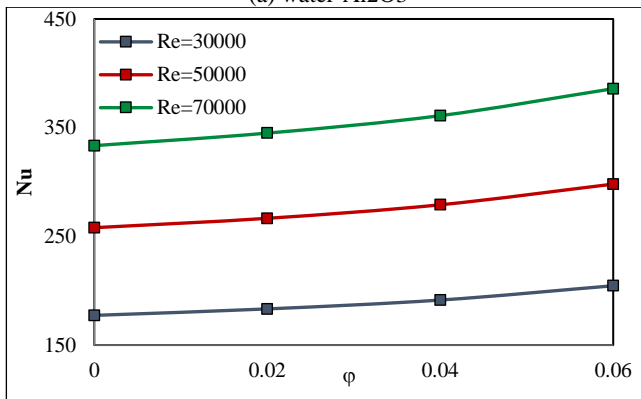




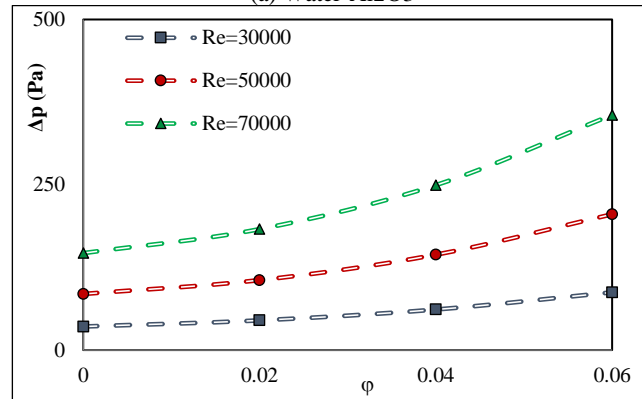
(a) water-Al<sub>2</sub>O<sub>3</sub>



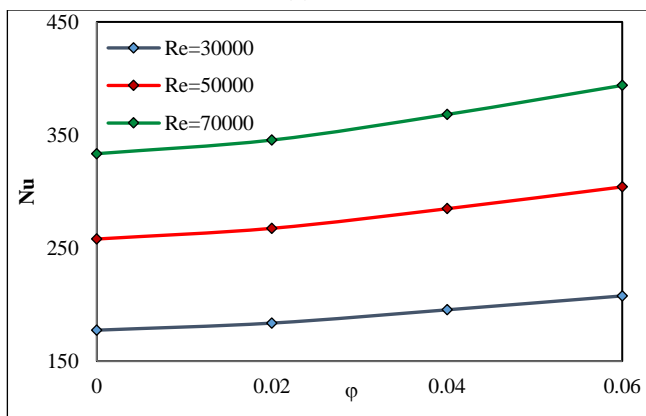
(a) Water-Al<sub>2</sub>O<sub>3</sub>



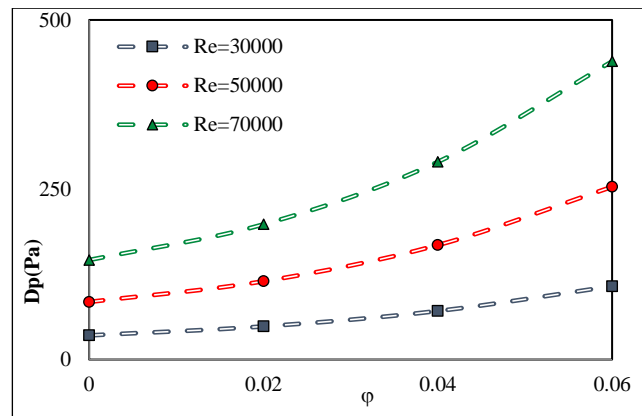
(b) Water-Cu



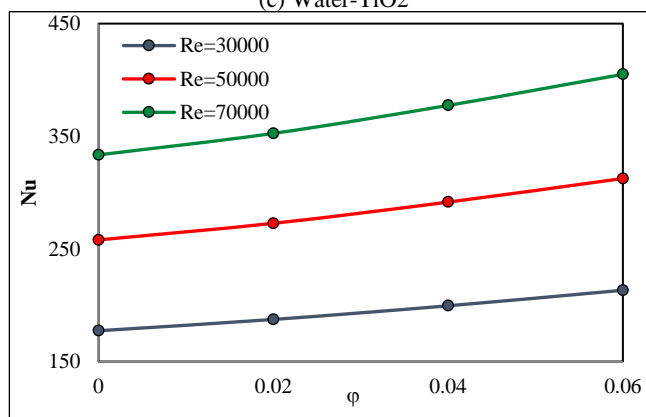
(b) Water-Cu



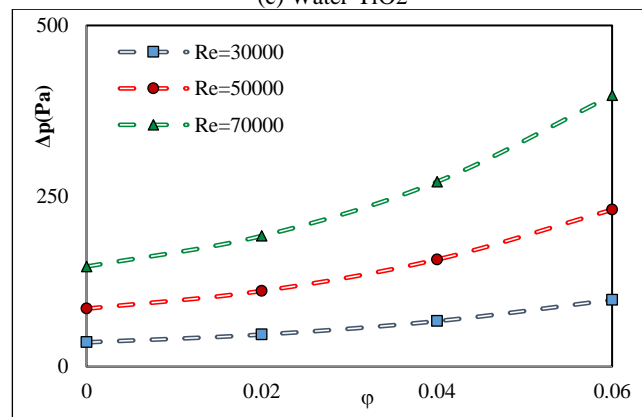
(c) Water-TiO<sub>2</sub>



(c) Water-TiO<sub>2</sub>



(d) Water-CuO



(d) Water-CuO

**Fig. 7.** Effect of particle loading on the Nu number for various Re numbers.

**Fig. 8.** Effect of particle loading on the pressure drop (Pa) for various Re numbers.

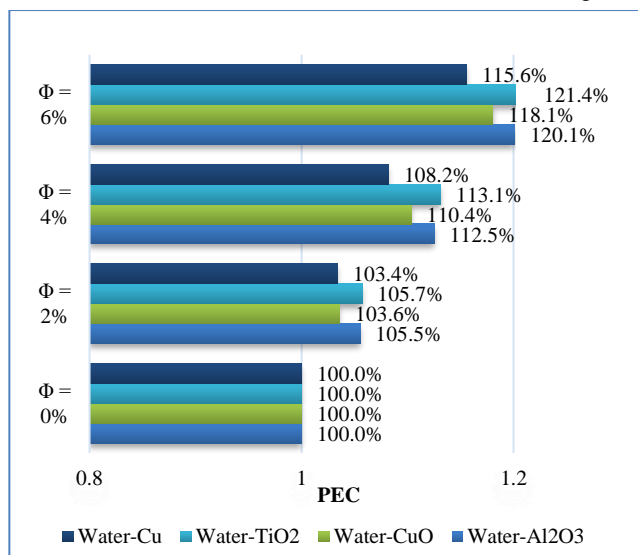


Fig. 9. The (PEC) of various nanofluids at Re= 70000 with different values of  $\phi$ .

## VII. CONCLUSION

Based on the literature, it can be concluded that the utilization of nanoparticles in base fluids for improving thermal properties is still an emerging field. The knowledge gap in literature is still considerable in terms of testing different types of nanoparticles with different volume fractions for conjugate heat transfer problems. Furthermore, there are still some open questions about the thermal-physical properties of nanofluids which thus requires further research. The current work tries to address this gap by studying the behavior of various nanofluids.

This paper presents results for the behavior of various nanoparticles mixed with water. Four different nanoparticles namely  $\text{Al}_2\text{O}_3$ ,  $\text{TiO}_2$ ,  $\text{CuO}$  and  $\text{Cu}$  were numerically tested in a uniformly heated receiver tube with different volume fractions at various Re numbers (30,000, 50000 and 70,000). Based on the results it can be concluded that water- $\text{TiO}_2$  is the best candidate for the nanofluids mixture as it has the highest Nu number profile and the lowest pressure drop compared to the other tested nanoparticles. At a volume fraction of 6% and Re = 70000, the Nu number enhancements of the nanofluids water- $\text{TiO}_2$ , water- $\text{Al}_2\text{O}_3$ , water- $\text{CuO}$  and water- $\text{Cu}$  were found to be 21.5, 20.2, 18.11 and 15.7% with the (PEC) of 1.214, 1.2, 1.18 and 1.155, respectively.

## VIII. ACKNOWLEDGMENT

The authors would like to thank the UK's Department of Business, Energy and Industrial Strategy for the financial support through Newton institutional links fund (Engineering Sustainable Solar Energy and Thermocline Alternatives-ESSEnTiAl, Grant ID 332271136). The authors would also like to thank the department of Mechanical, Aerospace and Civil Engineering (MACE), the University of Manchester for PhD scholarship of the first author.

## IX. REFERENCES

- [1] K. Khanafar, and K. Vafal, "A critical synthesis of thermophysical characteristics of nanofluids". International Journal of Heat and Mass Transfer, 2011, 54, pp. 4410-4428.
- [2] T. C. Paul, A. Morshed, E. B. Fox, and J. A. Khan, "Thermal performance of  $\text{Al}_2\text{O}_3$  Nanoparticle Enhanced Ionic Liquids (NEILs) for Concentrated Solar Power (CSP) applications". International Journal of Heat and Mass Transfer, 2015, 85, pp. 585-594.
- [3] P. Zadeh, T. Sokhansefat, A.B. Kasaeian, F. Kowsary, and A. Akbarzadeh, "Hybrid optimization algorithm for thermal analysis in a solar PTC based on nanofluid". Energy, 2015, 82, pp. 857-864.
- [4] A. Menbari, A. A. Alemrajabi, and Y. Ghayeb, "Investigation on the stability, viscosity and extinction coefficient of  $\text{CuO-Al}_2\text{O}_3/\text{Water}$  binary mixture nanofluid". Experimental Thermal and Fluid Science, 2016, 74, pp. 122-129.
- [5] A. Menbari, A. A. Alemrajabi, and A. Rezaei, "Experimental investigation of thermal performance for direct absorption solar PTC (DASPTC) based on binary nanofluids". Experimental Thermal and Fluid Science, 2017, 80, pp. 218-227.
- [6] Y. Wang, J. Xu, Q. Liu, Y. Chen, and H. Liu, "Performance analysis of a parabolic trough solar collector using  $\text{Al}_2\text{O}_3/\text{synthetic oil}$  nanofluid". Applied Thermal Engineering, 2016, 107, pp. 469-478.
- [7] A. Mwesigye, Z. Huan, and J.P. Meyer, "Thermal performance and entropy generation analysis of a high concentration ratio parabolic trough solar collector with  $\text{Cu-Therminol@VP-1}$  nanofluid". Energy Conversion and Management, 2016, 120, pp. 449-465.
- [8] A. Allouhi, M. Benzakour, R. Saidur, T. Kousksou, and A. Jamil, "Energy and exergy analyses of a parabolic trough collector operated with nanofluids for medium and high temperature applications". Energy Conversion and Management, 2018.
- [9] T. Aguilar, N. Javier, S. Antonio, I. Elisa, J. Juan, M. Paloma, G. Roberto, C. P. José, A. Rodrigo, and F. Concha, "Investigation of Enhanced Thermal Properties in  $\text{NiO}$ -Based Nanofluids for Concentrating Solar Power Applications: A Molecular Dynamics and Experimental Analysis". Applied Energy, 2018, 211, pp. 677-688.
- [10] M. Turkyilmazoglu, "Condensation of laminar film over curved vertical walls using single and two-phase nanofluid models". European Journal of Mechanics -B/Fluids, 2017, 65, pp.194-191.
- [11] L. Redjem, M. Ould-Rouiss, and G. Lauriat, "Direct numerical simulation of turbulent heat transfer in pipe flows: Effect of Prandtl number". International Journal of Heat and Fluid Flow, 2007, pp. 847-861.
- [12] B. Petukhov, "Heat Transfer and Friction in Turbulent Pipe Flow with Variable Physical Properties". Advance in heat transfer, 1970, V6, pp. 503-564.
- [13] V. Gnielinski, "New Equations for Heat and Mass Transfer in Turbulent Pipe and Channel Flow". International Chemical Engineering, 1976, pp. 359-368.